Machine Learning Techniques for elemental map analysis in MA-XRF Imaging

Theofanis Gerodimos[1], Ioannis Georvasilis[2], Anastasios Asvestas[1], Georgios P. Mastrotheodoros[1,3], Giannis Chantas[2], Aristidis Likas[2], Dimitrios F. Anagnostopoulos[1]

(1) Department of Materials Science and Engineering, University of Ioannina, Greece
(2) Department of Computer Science and Engineering, University of Ioannina, Greece
(3) Conservation of Antiquities & Works of Art Department, West Attica University, Greece

Introduction

X-ray fluorescence (XRF) spectrometry has been proven to be a core, non-destructive, analytical technique in cultural heritage studies, mainly because of its non-invasive character and ability to reveal the elemental composition of the analyzed artifacts rapidly. With the recent advances in scanning XRF spectrometers capable of attaining data on macroscopic dimensions (MA-XRF), XRF is excessively used for the in-situ analysis of works of art. Characteristic transition intensities extraction per pixel from the scanned images, signifying the elemental distribution, have nonlinear correlations with the measured spectra due to transitions overlapping, scattered radiation, and artifacts like escape peaks, pile-ups, and Bragg peaks. For this reason, elemental analysis requires time and human intervention with appropriate software [1]. To facilitate and improve data processing, we explore advanced machine learning techniques to predict elemental maps of the main elements of paintings scanned with M6 Jetstream (Bruker). We test and compare different architectures of neural networks (NN), like deep multilayered perceptron (MLP) and deep convolutional neural networks (CNN), to find the optimal model for achieving accurate prediction.

Data acquisition

In our experiment, spectra were collected with a MA-XRF scanner (M6 Jetstream, Bruker), as shown in Figure 1. The M6 Jetstream has a 30 W Rh X-ray tube with polycapillary optics. The present measurements were performed with a high voltage of 50 kV and a current of 600 μA. We scanned three religious panel paintings (dimensions of 536×404, 202×318, and 564×428 mm^2, respectively), and we collected about 500k spectra with a beam spot of 580 μm. We randomly used ~50k spectra to reduce the training time and improve our models' generalization. After, we tested our models using another painting (364×274 mm^2) shown in Figure 2.

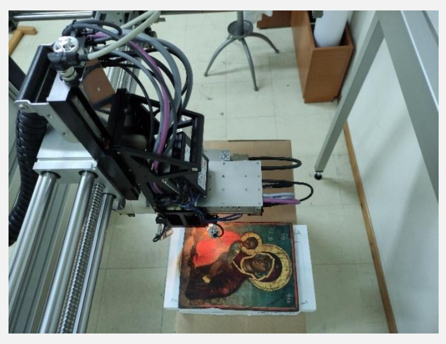

Figure 1: M6 Jetstream (Bruker) MA-XRF Scanner.

Figure 2: St John the Forerunner and a Hierarch.

Definition of models

In the first model, we tried a 1D classical CNN architecture. A CNN is a deep learning model commonly used in image processing and classification. We trained our model to predict the intensity for each one of 11 elements (S, K, Ca, Cr, Mn, Fe, Cu, Sr, Au, Hg, Pb) in the output, given the spectrum of each pixel as input. The architecture of the ConvNet we used is shown in Figure 3.

In the second model, we use a deep MLP architecture, shown in Figure 4. We implemented these two architectures to perform a comparative study between them and evaluate the role of convolution as data preprocessing in X-ray fluorescence spectra.

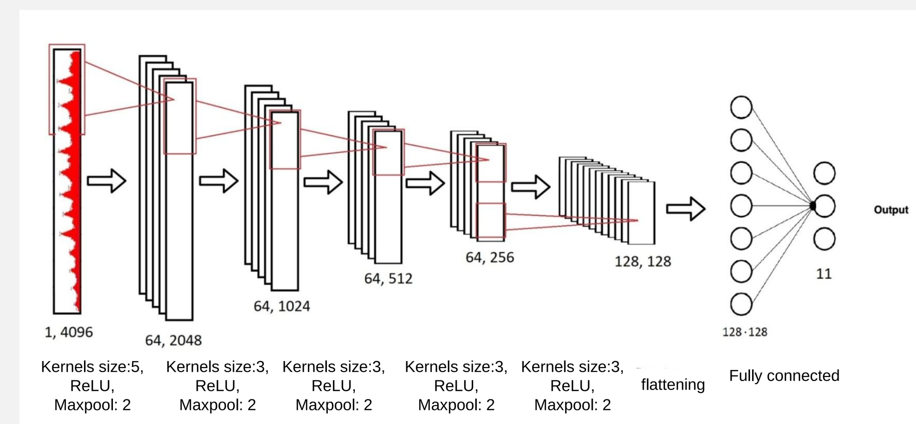

Figure 3: CNN architecture.

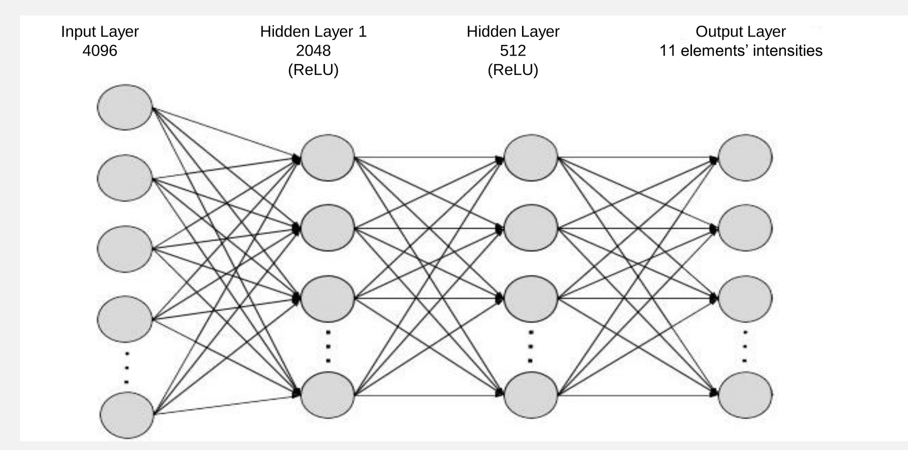

Figure 4: MLP architecture.

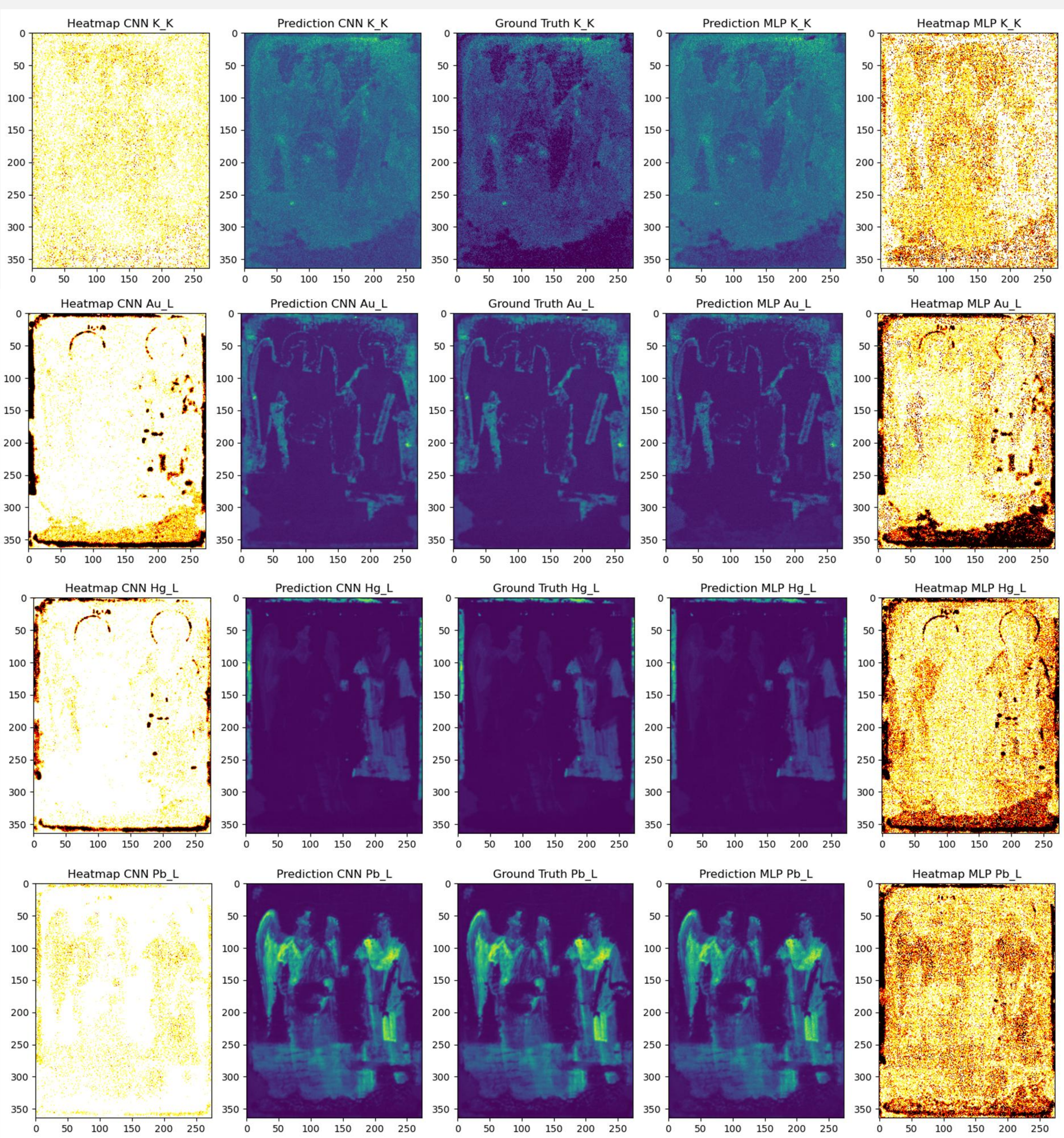

Figure 5: Heatmaps of z-score normalization, ground truth and prediction's elemental maps for K, Au, Hg, Pb.

Results

All models' performance was evaluated using K-Fold Cross Validation. The Dataset was partitioned into K different subsets that were subsequently used for testing the k-th trained model. Models' performance was obtained by the average of K testing scores. In Figure 5, we present the ground truth elemental map distribution of K, Au, Hg, and Pb in comparison to the results given by each model. To evaluate these results, firstly, we plot the distribution of the number of pixels per count for these four elements, as shown in Figure 6. Secondly, we compute the z-score normalization for the results of each model, as shown in the heat maps in Figure 5. Z-score normalization involves the rescaling of pixel values. It performs zero centering of data by subtracting the mean value from each pixel and dividing each dimension by its standard deviation, as given in Equation (1):

$$z = \left|\frac{X-\mu}{\sigma}\right|, (1)$$

The colors white, yellow, red and black correspond to abs(z) ≤ 1, abs(z) ≤ 2, abs(z) ≤ 3 and abs(z) > 3, respectively. Finally, we compute the Structural Similarity Index (SSIM) [2] between the ground truth and the predicted elemental map of each element as show in Table 1.

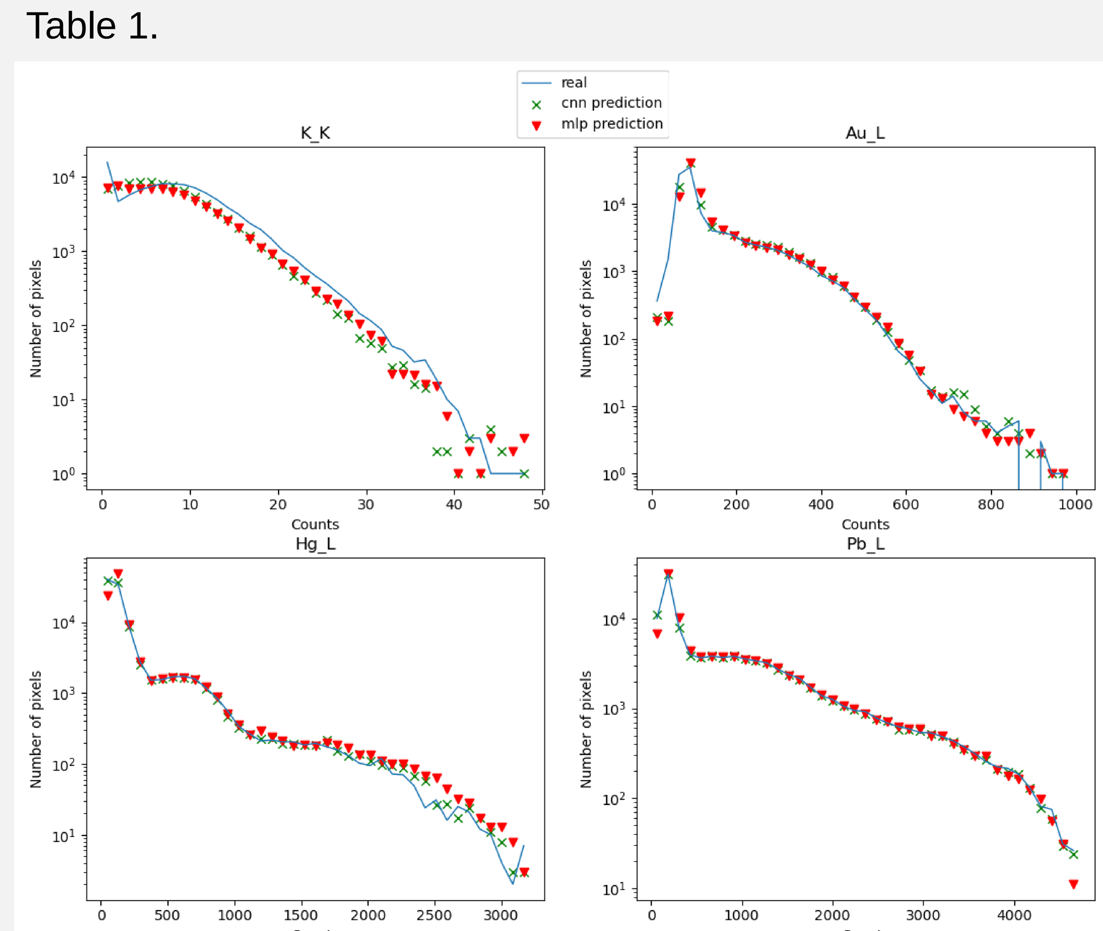

Figure 6: Distribution of number of pixels per counts interval.

Structural Similarity Index (SSIM)		
Element	CNN	MLP
S	0.99	0.66
K	0.80	0.57
Ca	0.99	0.90
Cr	0.99	0.88
Mn	0.97	0.78
Fe	1.00	0.94
Cu	0.98	0.90
Sr	1.00	0.87
Au	0.96	0.86
Hg	1.00	0.98
Pb	1.00	0.97

Table 1: SSIM between ground truth and prediction's elemental maps for all 11 elements. In red the elements shown in Fig. 5

Conclusions

In this work, we compare two artificial neural network architectures in the problem of elemental intensity distribution prediction through the XRF spectra without previous elemental analysis and human intervention. Convolution before linear layers seems to give better results. However, lower accuracy in both approaches is observed in low-intensity peaks and on energetically close peaks.

References

[1] Solé, V. A., Papillon, E., Cotte, M., Walter, P., & Susini, J. (2007). A multiplatform code for the analysis of energy-dispersive X-ray fluorescence spectra. *Spectrochimica Acta Part B: Atomic Spectroscopy*, *62*(1), 63-68.

[2] Wang, Z., Bovik, A. C., Sheikh, H. R., & Simoncelli, E. P. (2004). Image quality assessment: from error visibility to structural similarity. *IEEE transactions on image processing*, *13*(4), 600-612.

Acknowledgments

This research was supported by the project "Center for research, Quality analysis of cultural heritage materials and communication of science" (MIS 5047233) which is implemented under the Action "Reinforcement of the Research and Innovation Infrastructure", funded by the Operational Programme "Competitiveness, Entrepreneurship and Innovation" (NSRF 2014-2020) and co-financed by Greece and the European Union (European Regional Development Fund).

MA-XRF scanning in Conservation, Art and Archaeology 2022

3RD CONFERENCE ON THE USE OF XRF IMAGING IN CONSERVATION, ART AND ARCHAEOLOGY

MA-XRF 2022 26.09-27.09 DELFT (NL)

26-27 September 2022,

Museum Prinsenhof Delft, Netherlands

Co-financed by Greece and the European Union